AAPS PharmSciTech (2020) 21:313
DOI: 10.1208/s12249-020-01855-1

Research Article

Paclitaxel-Loaded Colloidal Silica and TPGS-Based Solid Self-Emulsifying System Interferes Akt/mTOR Pathway in MDA-MB-231 and Demonstrates Anti-tumor Effect in Syngeneic Mammary Tumors

Jaya Gopal Meher,[1] Shivani Dixit,[2] Yuvraj Singh,[1] Vivek K. Pawar,[1] Rituraj Konwar,[2] Ravi Saklani,[1] and Manish K. Chourasia[1,3]

Received 15 August 2020; accepted 14 October 2020

Abstract. A solid self-emulsifying drug delivery system (SEDDS) of paclitaxel (PTX) was developed that could enhance its oral bioavailability and neutralize other niggles associated with conventional delivery systems of PTX. TPGS-centered SEDDS containing PTX was optimized by Box-Behnken experimental design and then formulated as fumed colloidal silica–based solid SEDDS microparticles (Si-PTX-S-SEDDS). AFM analysis exhibited round-shaped microparticles of approximately 2–3 μM diameter, whereas after reconstitution, particle size measurement showed nanoemulsion droplets of 30.00 ± 2.00 nm with a zeta potential of 17.38 ± 2.88 mV. Si-PTX-S-SEDDS displayed improved efficacy proven by reduced IC_{50} of 0.19 ± 0.03 μM against MDA-MB-231 cells and a 45.83-fold higher cellular uptake in comparison to free PTX. Molecular mechanistic studies showed mitochondria-mediated intrinsic pathway of apoptosis following Akt/mTOR pathway, which is accompanied by survivin downregulation. Rhodamine 123 assay and chylomicron flow blocking studies revealed P-gp inhibition potential and lymphatic uptake of Si-PTX-S-SEDDS, responsible for over 4-fold increment in oral bioavailability compared to PTX administered as Taxol. *In vivo* anti-tumor studies in syngeneic mammary tumor model in SD rats revealed higher efficacy of Si-PTX-S-SEDDS as evident from significant reduction in tumor burden. In total, the developed Si-PTX-S-SEDDS formulation was found as an appropriate option for oral delivery of PTX.

KEY WORDS: paclitaxel; solid SEDDS; breast cancer; Akt/mTOR pathway; apoptosis.

INTRODUCTION

Paclitaxel (PTX) is a first-line anticancer agent used for chemotherapy in breast cancer treatment. Owing to its extreme hydrophobicity, it is needed to be administered intravenously as emulsion formulation, Taxol that comprises ethanol and Cremophor as excipients. However, there are profound concerns associated with PTX chemotherapy in its currently available marketed formulations like deleterious side effects and subpar therapeutic efficacy due to development of drug resistance. All these together jeopardize its clinical utility (1,2). Its administration *via* oral route could not be thought of owing to its extreme aversion to aqueous media, degradation by metabolic enzymes present in gastro intestinal tract (GIT), and efflux by P-gp pump present inside the lumen of the gut. All together solving these issues seems difficult but learning from the success story of cyclosporine as SEDDS (Neoral®/Sandimmune® as SEDDS formulation for oral use), we hypothesized to make a novel SEDDS of PTX that could enhance its oral bioavailability and neutralize other niggles associated with conventional delivery systems of PTX. We also tried to engage some smart excipients that could take care of the P-gp efflux issue with PTX and thereby circumventing drug resistance, breaking the trend of silent excipients.

Based on our prior art of developing SEDDS formulations, we have selected a series of excipients with varying hydrophilic lipophilic balance (HLB) value to develop a suitable isotropic mixture, that could ultimately give rise to a stable nanoemulsion upon dilution with water. Further curtailing the issue of stability associated with conventional SEDDS, we have developed a solid SEDDS formulation. For this purpose, fumed colloidal silica was employed, which enjoys the privilege GRAS status from US-FDA and also widely used in pharmaceutical industries (3). For a better understanding of the effects of different process and product variables on the characteristics of end product (SEDDS), we

[1] Pharmaceutics and Pharmacokinetics Division, CSIR-Central Drug Research Institute, Lucknow, UP 226031, India.
[2] Endocrinology Division, CSIR-Central Drug Research Institute, Lucknow, UP 226031, India.
[3] To whom correspondence should be addressed. (e–mail: manish_chourasia@cdri.res.in)

Published online: 09 November 2020

have employed design of experiments (DoE) which has become a mandatory regulatory aspect these days (4). The developed formulation is fabricated contemplating the scope of scalability for industrial translation.

The developed solid SEDDS was further studied extensively to propound anticancer effect against MCF-7 and MDA-MB-231 cancer cells. Pharmacokinetic and pharmacodynamic intonation in PTX brought by developed SEDDS was studied on New Zealand white rabbit and Sprague Dawley rats, respectively. It was followed by detailed molecular mechanistic pathway studies. In the next sections, we have given a brief on the systematic methodologies adopted for the design, development, and evaluation of the solid SEDDS, results that are obtained from various experiments and also a brief on the discussion of the obtained results.

MATERIALS AND METHODS

Materials

MiliQ ultrapure water (Millipore, Milli-Q plus 185, Bedford, MA, US) was used to prepare various formulations, media, reagents, and buffers throughout the experiments. PTX was received as a generous gift sample from Intas Pharma, Ahmedabad, India. D-a-toco-pheryl polyethylene glycol succinate (TPGS), vitamin E, fumed colloidal silica, solvents, and other chemicals were purchased from Sigma Aldrich, St. Louis, MO, USA. Labrafac™ lipophile WL 1349, Gelucire®, and Capryol®90 were obtained as gift samples from Gattefosse, St-Priest, France. Cyclosporin (Graftin 100 mg Capsule, Ranbaxy Laboratories Limited, India) and Taxol were purchased from registered medical agencies, Lucknow, India. All the biochemicals and kits for *in vitro* cell culture studies and western blotting studies were purchased from Sigma Aldrich, St. Louis, MO, USA. All antibodies for western blotting studies were purchased from Cell Signaling Technology, USA.

Methods

Formulation and Optimization of SEDDS

By taking clue from the solubility studies in the preformulation investigations, and based on our prior art of developing SEDDS formulations, we have chosen the oil phase as a combination of vitamin E, TPGS, and Labrafac (3:1:1 weight ratio). The resultant oil phase had an HLB value of 6.44, desired for the development of a stable formulation. Taking this into consideration, we have selected Capryol® 90 and Gelucire® (4:1 weight ratio) as surfactant and co-surfactant system. Box-Behnken experimental (Design Expert 7.0.0, Stat-Ease, Inc., Trial version) design was utilized for further optimization of the formulation on the basis of size and PDI of the emulsion droplets (Table I). SEDDS were prepared by a mixing technique where melted TPGS was mixed with vitamin E followed by the addition of labrafac, Capryol® 90, and Gelucire® in exact order with constant stirring at 300 rpm (IKA® RCT Basic) for 15 min to obtain an isotropic mixture. PTX or dye-loaded SEDDS were prepared in the same manner with an additional step of mixing the drug or dye in the oily vehicle. The isotropic mixtures were stored in airtight vials for further studies.

Formulation of Solid SEDDS (Si-PTX-S-SEDDS)

The solid SEDDS (Si-PTX-S-SEDDS) formulation was developed by employing spray drying technology and using fumed colloidal silica as a solid carrier (5). Briefly, 5 ml of liquid SEDDS formulation was added dropwise in a 1% *w/v* solution of colloidal silica in ethanol, with constant stirring at 200 rpm for 10 min. The resultant mixture was subjected to spray drying with a mini-spray dryer (Büchi 190 nozzle-type, Flawil, Switzerland) of laboratory scale. The operating conditions are shown in Table II. The resultant powdered formulation was stored in amber-colored glass vials for further studies.

Solid-State Characterization

For solid-state characterization of the developed Si-PTX-S-SEDDS, the sample cells were purged with nitrogen at a flow rate of 25 mL/min and instrument was calibrated with high purity indium standard before processing the samples using DSC-Q200, TA Instruments, USA. Accurately weighed 3 mg of PTX and the Si-PTX-S-SEDDS were separately subjected to DSC scanning at a heating rate of 10°C/min in

Table I. Dependent and Independent Variables and Experimental Runs for Formulations and Optimization of SEDDS Employing Box-Behnken Experimental Design

Variables		Levels	
Independent variables		Low (−1)	High (+1)
A: oil phase		5	25
B: surfactant		4	12
C: co-surfactant		1	3
Dependent variables		Desirability	
R_1: droplet size (nm)		Minimize	
R_2: PDI		Minimize	
Experimental runs with excipients			
Run	A	B	C
1	05.00	04.00	02.00
2	25.00	08.00	01.00
3	15.00	08.00	02.00
4	05.00	08.00	01.00
5	05.00	08.00	03.00
6	05.00	12.00	02.00
7	15.00	08.00	02.00
8	15.00	04.00	01.00
9	15.00	04.00	03.00
10	15.00	08.00	02.00
11	25.00	04.00	02.00
12	25.00	12.00	02.00
13	15.00	12.00	03.00
14	15.00	12.00	01.00
15	15.00	08.00	02.00
16	25.00	08.00	03.00
17	15.00	08.00	02.00

A: oil phase; vitamin E:TPGS:Labrafac (3:1:1), B: Capryol®90, C: Gelucire, PDI poly dispersity index

Table II. Operating Conditions for Spray Drying of Colloidal Silica–Based SEDDS Formulations

• Name of instrument	:Büchi 190 nozzle-type, Flawil, Switzerland
• Pump	:Peristaltic pump
• Nozzle diameter	:0.70 mm
• Inlet temperature	:61°C
• Outlet temperature	:40°C
• Flow rate	:5 mL/min
• Air pressure	:4 kg/cm^2
• Aspirator pressure	:− 25 mbar

T_{zero} aluminum pans from 50 to 300°C. The DSC spectra were obtained and interpreted (5).

Physiochemical Characterization

The formulated Si-PTX-S-SEDDS was characterized for emulsification efficiency, mean droplet size, PDI, and zeta potential. The particle size of spray-dried Si-PTX-S-SEDDS was measured by employing laser diffraction technology of particle size analyzer (Malvern Mastersizer, 2000, UK), as per previously reported method (6). For evaluation of emulsification efficiency, the Si-PTX-S-SEDDS was added slowly to water at 37 ± 1°C with mild stirring. The time required by the formulation to get emulsified is noted (7). After reconstitution, particle size, zeta potential, and PDI of the formed nanoemulsion were measured by dynamic light scattering (DLS) technology employing Zetasizer (Nano ZS, Malvern Instruments, UK) (8).

Si-PTX-S-SEDDS Morphology Analysis

The topographic features of the developed Si-PTX-S-SEDDS were evaluated by atomic force microscope (APE Research, Italy) in non-contact mode. Briefly, the diluted formulation sample was carefully placed on a clean glass cover slip and allowed to dry under nitrogen flow at room temperature. Cantilevers with their corresponding properties were set and the formulation was scanned from a different field. The images were processed for 3D surface topography by the Gwyddion 2.3 software (9).

Drug Content Assay, Percent Yield, and Encapsulation Efficiency

For drug content assay, the Si-PTX-S-SEDDS was reconstituted with Milli-Q water and a quantified volume of formed microemulsion was dissolved in methanol and then analyzed. Percent yield of Si-PTX-S-SEDDS was determined by formula of ratio of actual yield to theoretical yield multiplied with hundred. For the determination of encapsulation efficiency, the reconstituted formulation was centrifuged at 12,000×*g* for 30 min (Sigma 3–18 K, SciQuip Ltd., UK) and the PTX in separated oil phase was diluted with methanol and analyzed. The concentration of PTX in the sample was determined by the RP-HPLC method previously reported by us (8).

In Vitro Drug Dissolution

USP type II (paddle type) dissolution apparatus was employed for *in vitro* drug dissolution studies. Accurately weighed Si-PTX-S-SEDDS formulation was placed into the dissolution vessels containing dissolution media (SGF pH 1.2 for 2 h, SIF pH 6.8 for 8 h, and pH 6.8 up to 24 h) which was maintained at 200 rpm and 37 ± 0.5°C. One percent V/V Tween 80 was added in dissolution media to maintain the sink condition (10). Taxol containing equivalent content of PTX was used as control to compare with the dissolution profile of the developed formulation. At pre-determined time points, aliquot samples were withdrawn and replenished with fresh dissolution media. Previously reported RP-HPLC method was used to estimate the amount of drug released at different time points (8).

Stability Studies

Si-PTX-S-SEDDS was stored in hermetically sealed glass containers and subjected to storage stability studies at two different temperature conditions, *i.e.*, 4 ± 2°C and 25 ± 2°C for 6 months. At predefined time intervals, any alteration in the mean droplet size, PDI, and zeta potential was examined (11).

Cytotoxicity and Cellular Uptake Studies

The *in vitro* cytotoxicity of Si-PTX-S-SEDDS was evaluated by MTT assay in human breast cancer cell lines, *viz* MCF-7and MDA-MB-231. The procedure followed by Gursoy *et al.* was adopted for the assay with minor modifications (12). Briefly, 1×10^4 cells per well were grown in 96-well culture plates and incubated in CO_2 (5%) incubator at 37°C. The old media was replaced with fresh media containing Si-PTX-S-SEDDS, Taxol, and blank Si-S-SEDDS with various equivalent concentrations of PTX (0.25 to 20 μM) after 24 h of incubation. The treated cells were incubated for 24 h, 48 h, and 72 h, after which the treatment was terminated by aspirating treatment media and replacing it with fresh media doped with MTT (0.5 mg/mL) for 4 h. Subsequently, DMSO was added to dissolve the formazan crystals and optical density of treated and untreated cells was measured (PowerWave XS, Biotek, VT, USA) at 570 nm. IC_{50} was determined by calculating percentage cell inhibition using non-linear regression analysis in GraphPad Prism (Version-5.01).

The *in vitro* cellular uptake of Si-S-SEDDS in cancer cells was examined by fluorescence-activated cell sorting (FACS) flow cytometry (8). Briefly, the Si-S-SEDDS formulation was incubated with FITC to obtain the FITC-loaded solid SEDDS formulation. Then, MDA-MB-231 cells (1×10^6 cells per well) were treated with FITC-loaded formulation in six-well culture plates. After incubation of 6 h, cells were washed with PBS (pH 7.4) and evaluated for fluorescence using Calibur flow cytometer (Becton, Dickinson, San Jose, CA, USA) equipped with ModFit LT 2.0 and Cell Quest software.

Wound Healing Assay

Wound healing assay was performed as per previously reported method with minor modifications (13). Briefly, MDA-MB-231 cells were seeded in six-well plates at a density

of 1×10^6 cells/well. When the cells were 90% confluent, a scratch was made at the middle of the wells followed by treatment with Si-PTX-S-SEDDS, Taxol, and blank Si-S-SEDDS (equivalent to 0.5 μM PTX) for 48 h. Cells were observed under phase-contrast microscope (Nikon, Japan) and wound areas were quantified by employing Image J (1.48v) software.

Cellular and Nuclear Morphology

Effect of Si-PTX-S-SEDDS on the cellular and nuclear morphology of MDA-MB-231 cells was studied by previously reported method of Yang *et al*. with minor modifications (14). Briefly, MDA MB-231 cells were seeded in 24-well culture plates and treated with Si-PTX-S-SEDDS, Taxol, and blank Si-S-SEDDS (equivalent to 1 μM PTX). After predefined, time points cells were washed with PBS (pH 7.4) and observed under phase-contrast microscope for any morphological changes. Similarly, for the nuclear morphology studies, MDA-MB-231 cells at a density of 2×10^4 cells/well were seeded in 24 well plates and treated as mentioned above. After the respective incubation, time cells were washed with PBS (pH 7.4), fixed in 4% para-formaldehyde, and permeabilized with 0.5% tritonX100. Fixed and permeabilized cells were stained with DAPI (0.5 μg/mL) and observed under fluorescence microscope (14).

Cell Cycle Analysis

Cell cycle phase arrest induced by developed formulation was studied in MDA-MB-231 cells as per standard protocol (8). Briefly, MDA-MB-231 cells were treated with Si-PTX-S-SEDDS, Taxol, and blank Si-S-SEDDS as mentioned above. After the respective incubation time, cells were processed and analyzed by flow cytometry to determine the phase of cell cycle arrest.

Annexin V-FITC Double Staining Assay

Cell death in MDA-MB-231 cells after treatment with solid SEDDS formulation was investigated by Annexin V-FITC apoptosis detection kit (Sigma Aldrich, USA) as per manufacturer's instructions. MDA-MB-231 cells were treated with Si-PTX-S-SEDDS, Taxol, and blank Si-S-SEDDS. The treated cells were trypsinized, centrifuged, washed with PBS, and re-suspended in DNA binding buffer (500 μL). After that, Annexin V-FITC (5 μL) and propidium iodide (5 μL) were added to the cells and after an incubation period of 30 min in dark, cells were analyzed by flow cytometry.

Mitochondrial Membrane Potential Analysis

Effect of treatment of solid SEDDS formulations in the mitochondrial membrane potential (MMP) of MDA-MB-231 cells was investigated by previously reported method with slight modifications (8). Briefly, cells were given treatment as mentioned in previous section and stained with JC-1 dye (5,5′,6,6′-Tetrachloro-1,1′,3,3′-tetraethyl-imidacarbocyanine iodide, 10 μg/mL, Sigma Aldrich). After an incubation period of 30 min, cells were analyzed for fluorescence intensity by flow cytometry.

Reactive Oxygen Species Generation

For detection of generation of reactive oxygen species (ROS) in MDA-MB-231 cells after treatment with solid SEDDS formulations, H_2DCFDA staining method was employed as per standard protocols (8).

Rhodamine 123 Accumulation Assay

P-gp inhibition was studied by rhodamine 123 accumulation assay in MDA- MB-231 cells. Briefly, cells were treated with (5 μM) Rhodamine 123 in the absence (negative control) or presence of the developed formulation. Cells treated with Verapamil (30 μM) were employed as positive control. After an incubation period of 2 h, cells were washed twice with PBS and fluorescence of Rhodamine 123 was quantified by employing flow cytometer (BD Biosciences, FACS Aria, Germany) at 485 nm (excitation) and 530 nm (emission) (15).

Effect of Si-PTX-S-SEDDS on Apoptotic Markers

Alteration in the expression of pro-apoptotic and anti-apoptotic proteins in MDA-MB-231 cells on treatment with the developed formulation was studied by western blotting technique. Cells were exposed to different treatment conditions as mentioned above and after 72-h treatment, cells were subjected to lysis in RIPA buffer for isolation of proteins. The obtained cell lysates were subjected to electrophoresis on a SDS-PAGE and further transferred on ImmunoBlot™ PVDF membrane (Millipore, USA). After that, PVDF membranes were blocked in 2% BSA (blocking buffer) for 1 h on rocker shaker and were probed with primary antibodies overnight at 4°C. Washing was done and membranes were incubated with HRP conjugated secondary antibodies for 3 h at room temperature. Bands for p-Akt, Akt, p-mTOR, mTOR, Bcl-2, c-caspase 3, Survivin, and P-gp were visualized using ECL (Millipore, USA) reagent in Chemidoc (GE Healthcare Lifesciences) and compared to control protein β-actin.

Pharmacokinetic Studies

The pharmacokinetic studies of Si-PTX-S-SEDDS were carried out in Female Sprague Dawley rats (220–250 g) with prior approval from institutional animal ethics committee, CSIR-CDRI, Lucknow, India. All the animals were kept in 12-h light-dark cycle at controlled temperature conditions. After the acclimatization period of 7 days, animals were randomly divided into 5 groups with 6 animals per group ($n = 6$). Chylomicron flow blocking study was also conducted to understand the transport mechanism of S-SEDDS. Treatments were given as group 1 (vehicle control oral), group 2 (Si-PTX-S-SEDDS; 20 mg/kg oral), group 3 (Taxol; 20 mg/kg oral), group 4 (Si-PTX-S-SEDDS; 20 mg/kg oral + cyclohexamide; 3 mg/kg ip), and group 5 (Si-PTX-S-SEDDS, 20 mg/kg oral + colchicine; 5 mg/kg ip). Blood samples (200 μL) were collected in heparinized tubes at pre-determined time intervals and then centrifuged (2000×*g* for 10 min) to separate plasma. Collected plasma samples were subjected to liquid-liquid extraction to extract PTX and analyzed using a RP-HPLC method as per our previously reported method. All the pharmacokinetic parameters were calculated using Win

Nonlin software (Pharsight Co., Mountain View, CA, USA) (8).

In Vivo Anti-tumor Studies

Syngeneic mammary tumor model was employed for *in vivo* anti-tumor efficacy studies of Si-PTX-S-SEDDS. Tumor was induced as per previously reported method and when the tumor acquired a size of 200–300 mm^3, animals were randomly divided into 4 different treatment groups containing 6 rats/group. The four groups were treated with normal saline (vehicle control), Taxol (PTX equivalent to 20 mg/kg), blank Si-S-SEDDS, and Si-PTX-S-SEDDS (PTX equivalent to 10 mg/kg) respectively by oral route every 4 days for 21 days. Length and width of the tumors were measured on every 5th day by a digital Vernier caliper and tumor volume was calculated. The excised tumors were processed to remove undesired tissues and skin parts from the tumor surface and then were weighed on a precision balance (Essae, Teraoka Pvt. Ltd., Bengaluru, India). Further tumors were stored group wise in 10% neutral buffered formalin for other biological evaluations (13,16).

Tumor Histopathology Evaluation

Excised tumors were processed for histological examination (17). Briefly formalin (10% in normal saline) fixed tissues were cut into small pieces and passed through steps of histological slide preparation, *viz* dehydration, paraffin embedding, section cutting, deparaffinizing, rehydrating, and staining with hematoxylin and eosin (H & E). The stained sections were mounted with Dibutylphthalate Polystyrene Xylene (DPX) mounting medium and observed under light microscope to study treatment-induced histopathological changes in tumor.

Apoptosis in Tumor Tissues

To investigate the apoptosis in tumor tissues, TUNEL assay was performed (18). Tumor tissues from different treatment groups including the control group were processed for paraffin embedding and then cut into 5 μM thick sections. The processed sections were examined for apoptotic cells employing terminal deoxy-nucleotidyl transferase–mediated dUTP nick-end labeling (TUNEL) assay kit (Promega Corporation, USA) as per manufacturer's instructions. Furthermore, these sections were observed under confocal microscope (Olympus, BX61-FV1200-MPE, with FV1200 software module, 60X) to detect the TUNEL-positive cells and the images were captured for interpretation.

Lung Metastasis Evaluations

On the termination day of *in vivo* efficacy studies, lungs of the tumor-bearing SD rats were dissected and washed with PBS to remove any traces of blood and other tissues. Lungs were transferred to a vessel containing Bouin's solution and kept undisturbed at room temperature. After 72 h of storage, lungs stained with Bouin's fluid were observed under a stereoscopic microscope for the presence of metastatic nodules. The metastatic lesions appeared whitish whereas lung tissue stained yellow (19).

Statistical Analysis

One-way analysis of variance (ANOVA) was performed to calculate the level of significance employing Graph Pad Prism 5.01 (Graph Pad Software Inc., CA, USA). The level of statistical significance was expressed as $*p$ □ 0.05, $**p$ □ 0.01, and $***p$ □ 0.001. Statistical significance is shown in the "Results" section as and when required.

RESULTS

Formulation and Optimization

Based on the preliminary trials and calculated required HLB values, range of excipients were set and for a scientific approach in formulation and optimization we have used Box-Behnken experimental design. The 3 factors (independent variables), *viz* factor 1; oil phase, factor 2; surfactant (Capryol® 90), and factor 3; co-surfactants Gelucire®, were investigated for their effect on the dependent variables, *viz* R_1; droplet size and R_2; PDI. The desirable effect was to minimize the dependent variables to its lower level at a suitable combination of independent variables. With this input, the applied design proposed a set of 17 runs with all possible combination of the excipients. Table III gives the experimental findings of the dependent variables R_1 (droplet size) and R_2 (PDI) for the 17 different SEDDS formulations.

It could be observed that the range of R_1 (droplet size) was from 28.55 to 75.48 nm and the R_2 (PDI) was 0.208 to 0.786. A total of five SEDDS formulations could develop droplet size below 50 nm and at the same time four SEDDS were within 0.3 PDI. Based on these formulation results, the design was evaluated and optimized formulation was derived. Figure 1 gives the contour plots and 3D response surface plots showing the effect of excipients on the dependent variables. The polynomial equations derived for the correlation of both dependent and independent variables are shown below.

$$R_1\ (\text{droplet size}) = +53.67 + 7.57\text{A} - 13.32\text{B} - 1.69\text{C} + 2.75\text{AB} + 3.07\text{AC} + 0.59\text{BC} + 5.60\text{A}^2 - 0.10\text{B}^2 - 3.15\text{C}^2$$

$$R_2\ (\text{PDI}) = +0.50 + 0.025\text{A} - 0.088\ \text{B} - 0.030\ \text{C} + 0.11\ \text{AB} + 0.088\ \text{AC} + 0.022\ \text{BC} + 0.088\ \text{A}^2 - 0.089\ \text{B}^2 - 0.072\ \text{C}^2$$

Analysis of variance was employed along with multiple correlation (R^2) and the obtained p value for both the dependent variables R_1 and R_2 was found to be less than 0.0001. The results indicated that at low concentration of oil

Table III. The Dependent Variables; R_1: Droplet Size and R_2: PDI for the Proposed Experimental Runs with Combinations of Excipients from Box-Behnken Experimental Design

	Dependent variables	
Runs	R_1: droplet size (nm)	R_2: PDI
1	75.48	0.786
2	60.09	0.452
3	58.22	0.564
4	50.26	0.542
5	46.00	0.413
6	28.55	0.208
7	52.26	0.672
8	61.25	0.443
9	51.44	0.230
10	55.10	0.442
11	84.28	0.588
12	48.35	0.432
13	40.75	0.289
14	48.22	0.412
15	50.22	0.552
16	68.12	0.674
17	52.55	0.289

phase, when we move from low to high level of Capryol® 90, the droplet size decreases from 60 to 34 nm at a constant level of Gelucire®, whereas at the high level of oil phase, similar trend was observed; however, droplet size was comparatively higher and the reduction was from 75 to 50 nm. Similarly, when the concentration of oil phase was increased at constant level of Capryol® 90 and Gelucire®, there was an increase in droplet size from 60 to 75 nm. Similarly, in the PDI also, at low concentration of oil phase when we moved from low to high concentration of Capryol® 90, there was a decrease in PDI from 0.672 to 0.295 at constant level of Gelucire®. In the contrary, at higher level of oil phase, the PDI was increased from 0.508 to 0.538 with the increase in Capryol® 90 at constant level of Gelucire®. Based on all these interactions between excipients and their effect on droplet size and PDI of the SEDDS formulation, the software predicated the theoretical values for droplet and PDI at fixed concentration of excipients. For the present set of experiments, it was found that the proposed values were droplet size; 28.51 nm, PDI; 0.124 at oil phase; 5.35, Capryol® 90; 11.94, and Gelucire; 3.00 with a desirability function of 1. Taking this as an instruction, we have formulated a SEDDS formulation and the obtained droplet size and PDI were 25.86 nm and 0.208, respectively. As there was no significant difference between predicted values and obtained values, the experimental design model was found to be suitable for the present investigation. After formulation development and optimization of the conventional liquid SEDDS, the solid SEDDS (Si-PTX-S-SEDDS) was formulated by spray drying with a mini-spray dryer with fumed colloidal silica.

In Vitro Pharmaceutical Characterization

The spray-dried Si-PTX-S-SEDDS were evaluated for solid-state characteristics of the incorporated drug PTX. Figure 2a shows the DSC thermogram of both PTX and the Si-PTX-S-SEDDS. A sharp endothermic peak was observed near 223°C corresponding to the melting point of PTX suggesting the crystalline nature of the drug in its pure form, while the endothermic peak was observed to be disappeared in the Si-PTX-S-SEDDS formulation which indicates that the encapsulated PTX was in its amorphous form inside the formulation.

The particle size of the microparticles was found to be 2 ± 1 μM as analyzed from the Mastersizer (Fig. 2b). Topographic analysis from the atomic force microscope (AFM) revealed regular round-shaped particles with particle diameter of approximately 2–3 μM that are in close agreement with the results of particle size analysis obtained from Mastersizer (Fig. 2c). The emulsification time of the optimized Si-PTX-S-SEDDS was found to be 1.5 ± 0.40min. After reconstitution of Si-PTX-S-SEDDS, the droplet size of the formed nanoemulsion was found to be 30.00 ± 2.00 nm, PDI was 0.198 ± 0.050, and zeta potential was 17.38 ± 2.88 mV as analyzed by DLS, Zetasizer.

The percent yield, drug content, and encapsulation efficiency of the same formulation were determined to be 84.00 ± 4.68%, 98.46 ± 2.75%, and 95.63 ± 3.36%, respectively. The *in vitro* drug release profile of PTX from Si-PTX-S-SEDDS formulation is shown in Fig. 2d which showed that after 24 h, Taxol released 53.75 ± 5.21% and Si-PTX-S-SEDDS released 32.89 ± 3.00% of their respective PTX content into the dissolution medium. Obtained drug release data were fitted into various release kinetic models. The Si-PTX-S-SEDDS was found to follow Higuchi model (R^2; 0.9788), indicating a diffusion type of controlled release of PTX from the nanoemulsion core.

Stability

Storage stability of the Si-PTX-S-SEDDS was studied at room temperature and refrigerated condition. The results depicted in Table IV suggest good storage stability with no significant changes in the droplet size, zeta potential, or emulsification time over a period of 6 months.

In Vitro Cytotoxicity

Cytotoxic activity of Si-PTX-S-SEDDS, Taxol, and blank Si-S-SEDDS was investigated in breast cancer cell lines MCF-7 and MDA-MB-231 cells. In both the cells, SEDDS formulation exhibited strong cytotoxicity and it was observed to be more cytotoxic to MDA-MB-231 cells compared to MCF-7 cells. In comparison to Taxol, Si-PTX-S-SEDDS exhibited significantly lower IC_{50} (p 0.05) in MDA-MB-231 cells after a treatment period of 72 h. Blank Si-S-SEDDS formulation showed cytotoxicity at very high concentrations (IC_{50} 500 μM) in both the cancer cell lines. Figure 3 displays the cytotoxic effect of all treatments against MDA-MB-231 cells at different time points.

Treatment-induced alterations in cellular morphology were studied in MDA-MB-231 cells and revealed that both the Si-PTX-S-SEDDS and Taxol treatment cause membrane blebbing, shrinkage, and rounding of the cells (Fig. 3d). In the DAPI-stained cells, control cells showed intact nuclear

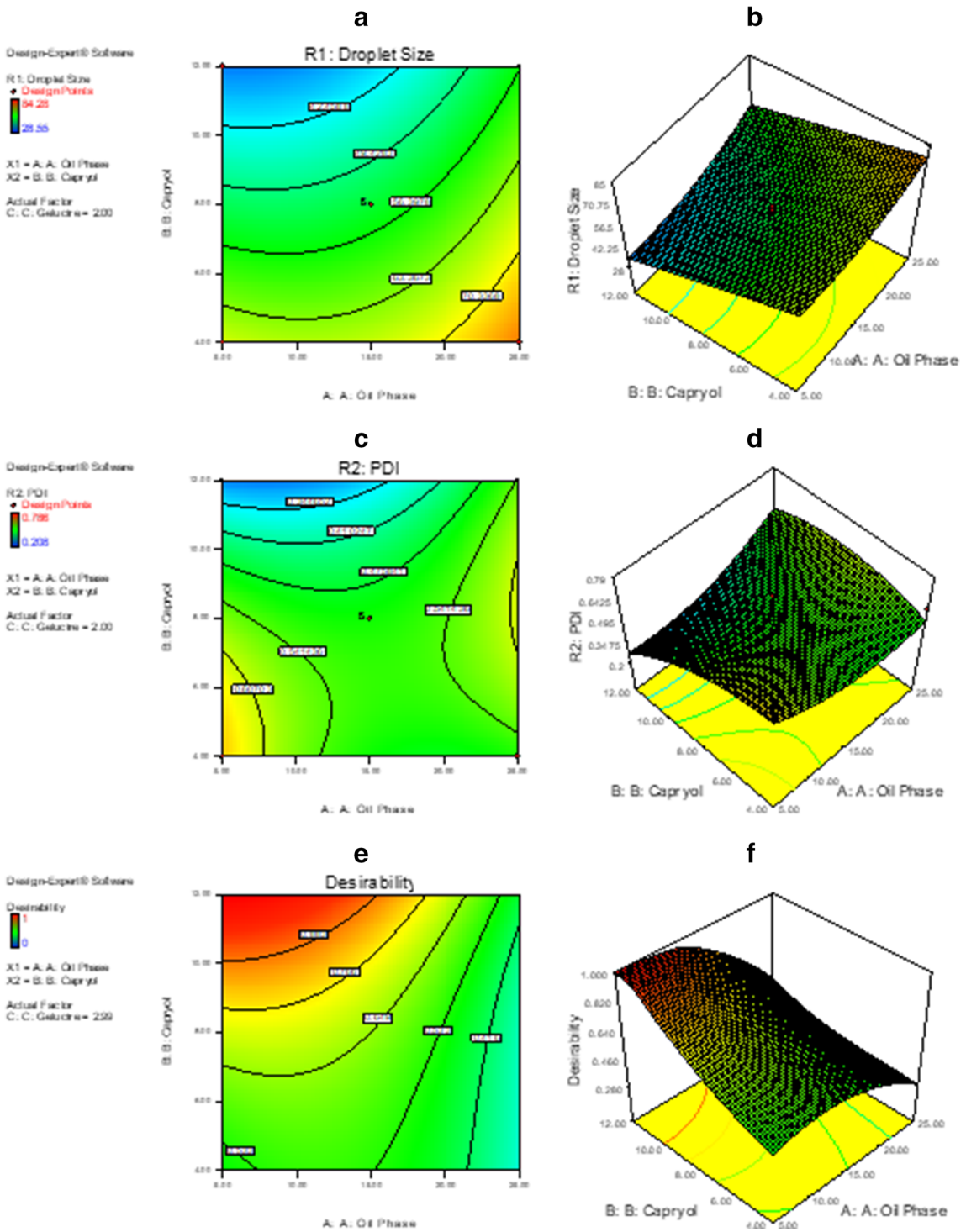

Fig. 1. **a** Contour plot and **b** 3D response surface plot showing the effect of oil phase, surfactant, and their interactions on R_1 (droplet size) at a fixed level of co-surfactant. **c** Contour plot and **d** 3D response surface plot showing the effect of oil phase, surfactant, and their interactions on R_2 (PDI) at a fixed level of co-surfactant. **e** Contour plot and **f** 3D surface plot showing the desirability function proposed by Box-Behnken experimental design

content, but Si-PTX-S-SEDDS- and Taxol-treated cells showed fragmented nuclei (Fig. 3e).

Figure 3f represents the treatment-induced effect on the wound healing tendencies of MDA-MB-231 cells. The cellular migration of MDA-MB-231 cells after treatment with Si-PTX-S-SEDDS was significantly reduced in all the treated cells. It was observed that in comparison to the control treatment, Si-PTX-S-SEDDS (p 0.001), Taxol (p 0.01), and blank Si-S-SEDDS (p 0.01) exhibited a significant difference in relative wound closure indicating the cytotoxic potential of the developed SEDDS formulations.

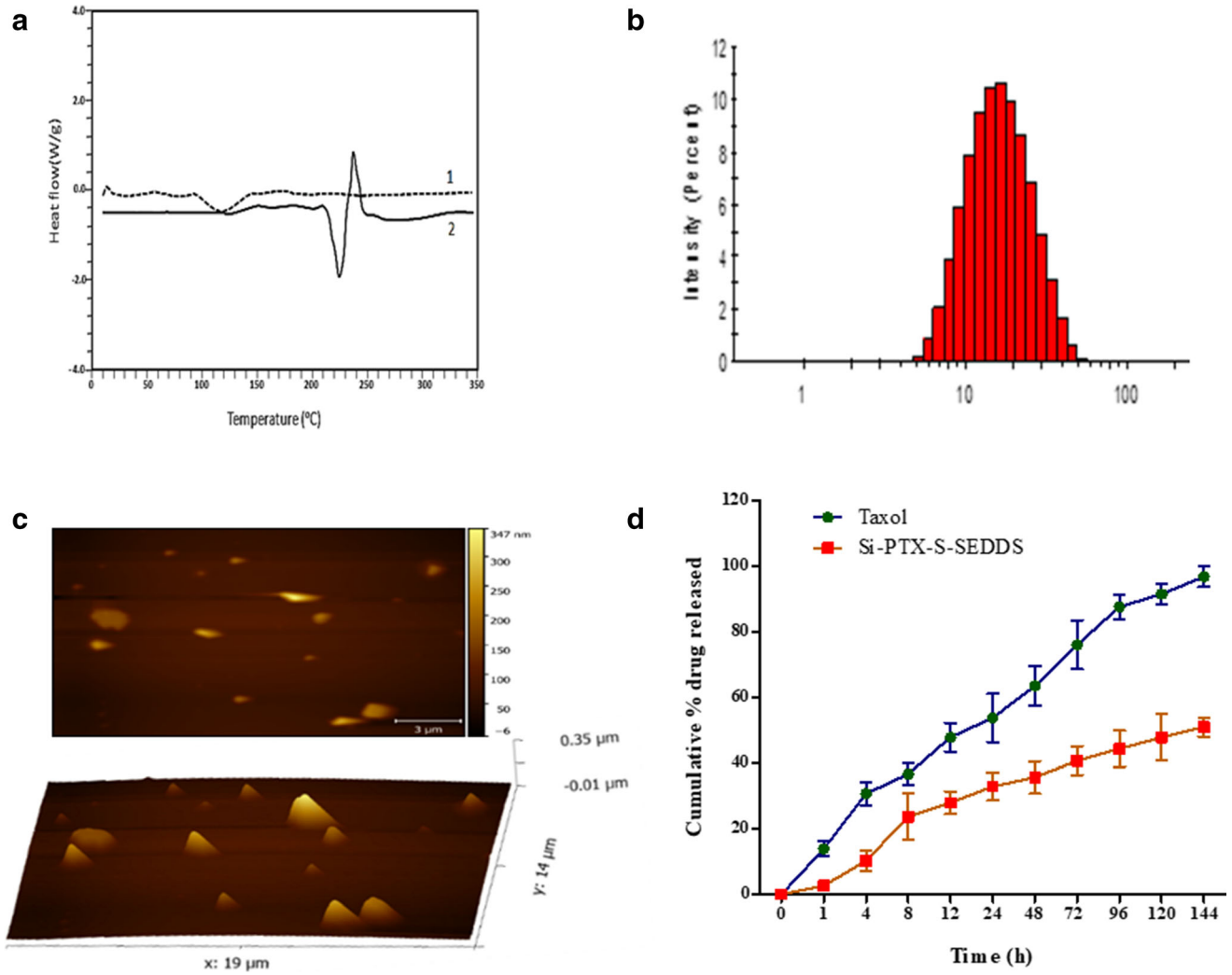

Fig. 2. Physiochemical characterization of Si-PTX-S-SEDDS formulation. **a** Differential scanning calorimetric thermogram of (1) Si-PTX-S-SEDDS and (2) PTX showing the solid-state characteristics of PTX in the formulation as well as in its pure form. **b** DLS graph displaying the droplet particle size distribution. **c** AFM photomicrograph exhibiting topographical features of Si-PTX-S-SEDDS particles. **d** *In vitro* release profile of PTX from Si-PTX-S-SEDDS in comparison to Taxol formulation

Table IV. Storage Stability Evaluation of Si-PTX-S-SEDDS for Mean Droplet Diameter, PDI, and Zeta Potential at 4 ± 2°C and 25 ± 2°C During 6 Months of Storage

Storage temperature	Characterization parameters*	Storage time (months)/values of evaluation parameters		
		Zero	Three	Six
4 ± 2°C	Droplet size (nm)	30.00 ± 2.00	31.56 ± 2.99	32.08 ± 1.86
	PDI	0.198 ± 0.050	0.176 ± 0.067	0.209 ± 0.012
	Zeta potential (mV)	− 17.38 ± 2.88	− 19.45 ± 1.44	− 18.53 ± 1.64
	Emulsification time (min)	1.5 ± 0.40	1.8 ± 0.20	1.6 ± 0.22
25 ± 2°C	Droplet size (nm)	30.00 ± 2.00	32.08 ± 1.87	32.77 ± 1.94
	PDI	0.198 ± 0.050	0.205 ± 0.018	0.200 ± 0.046
	Zeta potential (mV)	− 17.38 ± 2.88	− 17.88 ± 1.43	− 20.18 ± 2.36
	Emulsification time (min)	1.5 ± 0.40	1.6 ± 0.33	1.5 ± 0.79

**Mean ± SEM (n = 3)*

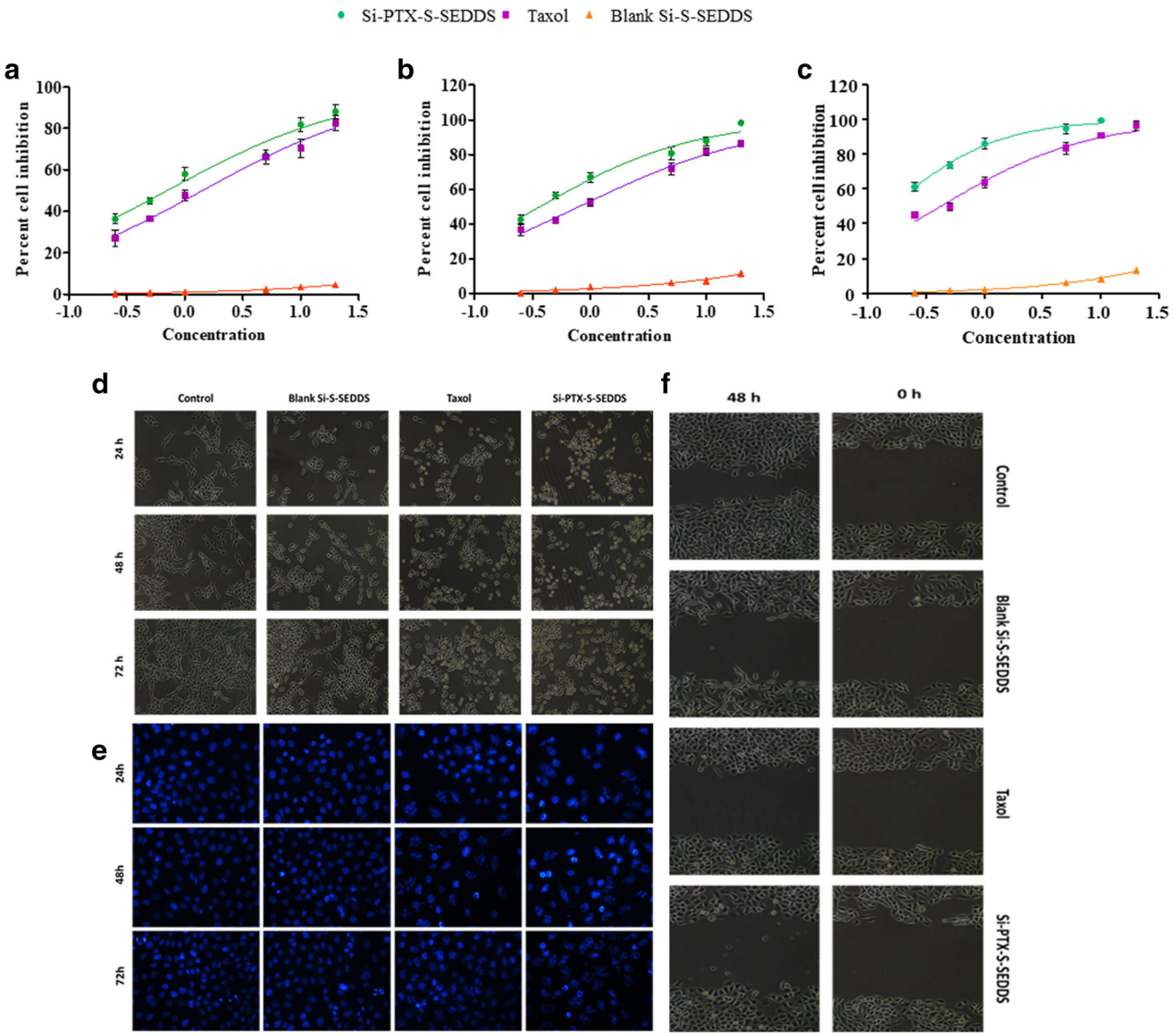

Fig. 3. *In vitro* cytotoxicity. Treatment-induced cytotoxicity represented as percent cell inhibition in MDA-MB-231 cell lines after an exposure of **a** 24 h, **b** 48 h, and **c** 72 h. Effect of different treatments on **e** cell morphology and **b** nuclear morphology and **f** wound healing of MDA-MB-231 cells

Cell Uptake Study

In vitro cell uptake of FITC-loaded SEDDS in MDA-MB-231 cells was investigated by flow cytometry analysis shown in Fig. 4a. It was observed that developed SEDDS formulation–assisted cell uptake of FITC was 45.83-fold higher in comparison to free FITC (control group).

Treatment-Induced Rhodamine 123 Accumulation by Si-PTX-S-SEDDS

Inhibition of P-gp expression in MDA-MB-232 cells was studied by Rhodamine 123 accumulation assay. Figure 4b exhibits the flow cytometry plots showing the treatment-induced changes in mean fluorescence intensity (MFI) associated with Rhodamine 123 accumulation in MDA-MB-231 cells. All the treatments, *viz* blank Si-S-SEDDS, Taxol, Verapamil, and Si-PTX-S-SEDDS, exhibited higher accumulation of Rhodamine 123 in MDA-MB-231 cells compared to control treatment. The MFI of blank Si-S-SEDDS was measured to be 112.00 ± 9.89 which was significantly higher (p 0.01) than the control-treated cells (27.50 ± 3.53). At the same time, the MFI of Si-PTX-S-SEDDS was noted to be 110.00 ± 19.80 that is significantly higher (p 0.01) than the control cells. Taxol also exhibited a higher MFI, *i.e.*, 79.00 ± 12.73 that was also a significant (p 0.05) increase in Rhodamine accumulation than the control cells. There was no significant difference in the MFI of both Si-PTX-S-SEDDS and Si-S-SEDDS formulations.

We monitored alteration in expression of well-established pro-apoptotic and anti-apoptotic proteins in MDA-MB-231 cells on treatment with the developed SEDDS formulation. The western blots of the proteins are shown in Fig. 4c. It could be observed that the expression of pro-

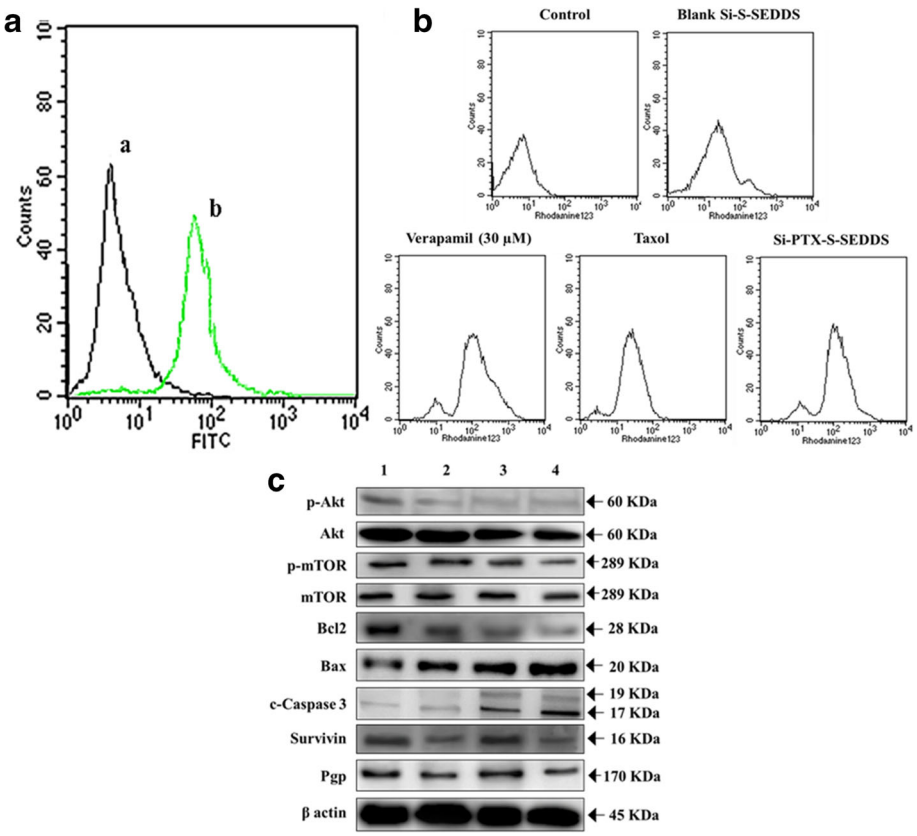

Fig. 4. **a** FACS histogram displaying florescence intensity corresponding to quantitative cell uptake of FITC-loaded (a) SEDDS formulation by MDA-MB-231 cells in comparison to (b) control cells. **b** Flow cytometry plots exhibiting the treatment-induced changes in fluorescence intensity associated with Rhodamine 123 accumulation in MDA-MB-231 cells. **c** Western blot results showing alteration in the expression of pro-apoptotic and anti-apoptotic proteins in MDA-MB-231 cells on treatment with (1) PBS (control), (2) blank Si-S-SEDDS, (3) Taxol, and (4) Si-PTX-S-SEDDS

apoptotic proteins like c-caspase 3 and Bax was upregulated in groups treated with the SEDDS formulation. Results demonstrated that in the Si-PTX-S-SEDDS-treated cells, expression of anti-apoptotic markers, *viz* Akt, mTOR, Bcl2, and their phosphorylated forms, was reduced. Survivin a well-established member of inhibitor of apoptosis (IAP) family was found to be overexpressed in cells treated with Taxol; however, the expression of survivin was significantly reduced in Si-PTX-S-SEDDS-treated cells compared to control cells ($p < 0.05$). As anticipated from the results of rhodamine assay, the expression of P-gp was found to be downregulated significantly in cells treated with the SEDDS formulation (p 0.01) compared to control group's cells.

Cell Cycle Distribution

Si-PTX-S-SEDDS and Taxol were observed to arrest the cell cycle in G_2M phase in MDA-MB-231 cells. Highest G_2M phase arrest was exhibited by Si-PTX-S-SEDDS, *i.e.*, 86.96 ± 1.37% (Fig. 5a) after 72 h of exposure. In comparison to the Taxol, Si-PTX-SEDDS exhibited significantly (p 0.001) higher G_2M phase arrest in all three time points. Blank formulations showed G_0/G phase arrest which was significantly higher (p 0.001) than control-treated cells.

Apoptosis

Annexin V-FITC assay showed a significantly (p 0.001) higher apoptotic populations of MDA-MB-231 cells treated with Si-PTX-S-SEDDS in comparison to Taxol (Fig. 5b). Highest total apoptosis was noted to be 63.05 ± 2.88% by Si-PTX-S-SEDDS after 72 h. Blank Si-S-SEDDS also caused apoptosis (16.41 ± 1.16%) that was significantly higher (p 0.05) than control treatment in MDA-MB-231 cells.

Mitochondrial Membrane Potential Alteration

Mitochondrial membrane potential in MDA-MB-231 cells was disrupted upon treatment with formulations where the Si-PTX-S-SEDDS exhibited significantly (p 0.01) higher disruption than Taxol (Fig. 5c). After 72 h of treatment exposure, Si-PTX-S-SEDDS showed 59.12 ± 1.39% green fluorescence which was highest in all treatment groups. Blank Si-S-SEDDS also showed significantly higher (p 0.01) green fluorescence than control.

Reactive Oxygen Species Production

H_2DCFDA staining assay revealed increase in production of ROS in MDA-MB-231 cells in all treatment groups

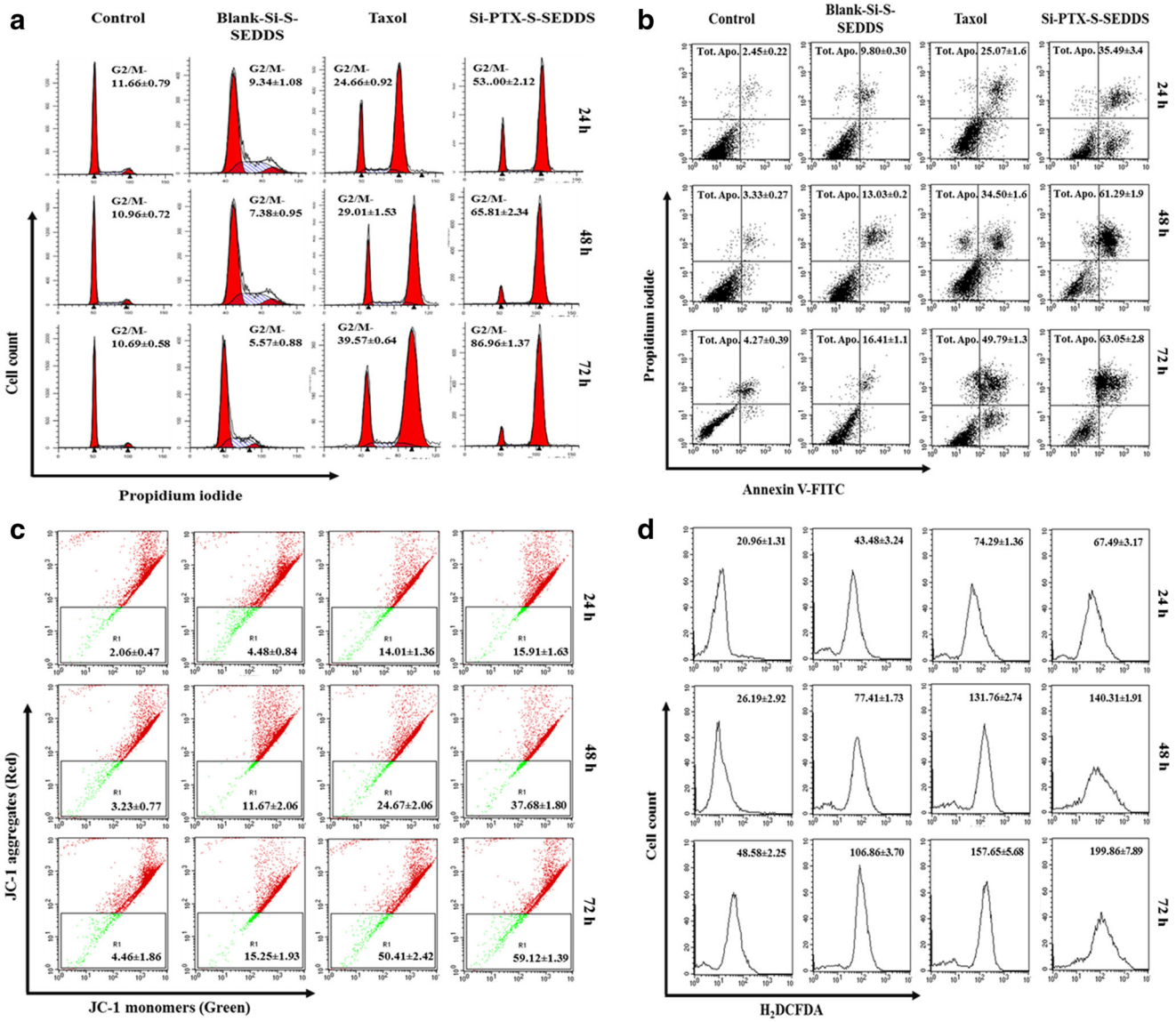

Fig. 5. Flow cytometry plots displaying the effect of different treatments on **a** cell cycle distribution and **b** apoptosis and **c** mitochondrial membrane potential and **d** ROS generation in MDA-MB-231 cells after 24 h, 48 h, and 72 h of treatment exposure

(Fig. 5d). Si-PTX-S-SEDDS treatment resulted in ~ 1.2-fold higher ROS generation compared to Taxol treated cells (p 0.001) after 72 h of exposure. Furthermore, blank Si-S-SEDDS also showed a significant increase (p 0.001) in ROS generation compared to control group after 72 h of treatment.

Pharmacokinetics and Lymphatic Uptake Study

The plasma pharmacokinetic parameters were investigated in Sprague Dawley rats. The plasma drug concentration and time profile of PTX after oral administration of Si-PTX-S-SEDDS is shown in Fig. 6 and the pharmacokinetic parameters are shown in Table V. It could be observed that the oral bioavailability of PTX was 21.32 ± 1.86% when administered as Si-PTX-S-SEDDS, whereas it was 4.28 ± 0.42% with Taxol formulation. When Si-PTX-S-SEDDS was administered after ip injection of chylomicron flow inhibitors, *viz* cycloheximide and colchicine, the oral bioavailability of the same was found to be significantly (p 0.01) decreased to 4.39 ± 0.69% and 3.54 ± 1.02%, respectively.

In Vivo Anti-tumor Efficacy

Tumor Volume

The LA-7 tumor-bearing SD rats were administered with saline (vehicle control), Taxol, blank Si-S-SEDDS, and SI-PTX-S-SEDDS and tumor volume was monitored. Results are summarized in Fig. 7. It was quite discernible that Taxol, blank SEDDS, and PTX-loaded SEDDS formulation treatment significantly hindered tumor growth compared to vehicle control treatment group (Fig. 7a). At the end of the study, tumor was excised and weighed to calculate the tumor burden. It was found that in Taxol- and Si-PTX-S-SEDDS-treated SD rats, the weight of the tumor was 3.11 ± 0.99 g and 0.82 ± 0.18 g, respectively. There was a significant (p 0.001)

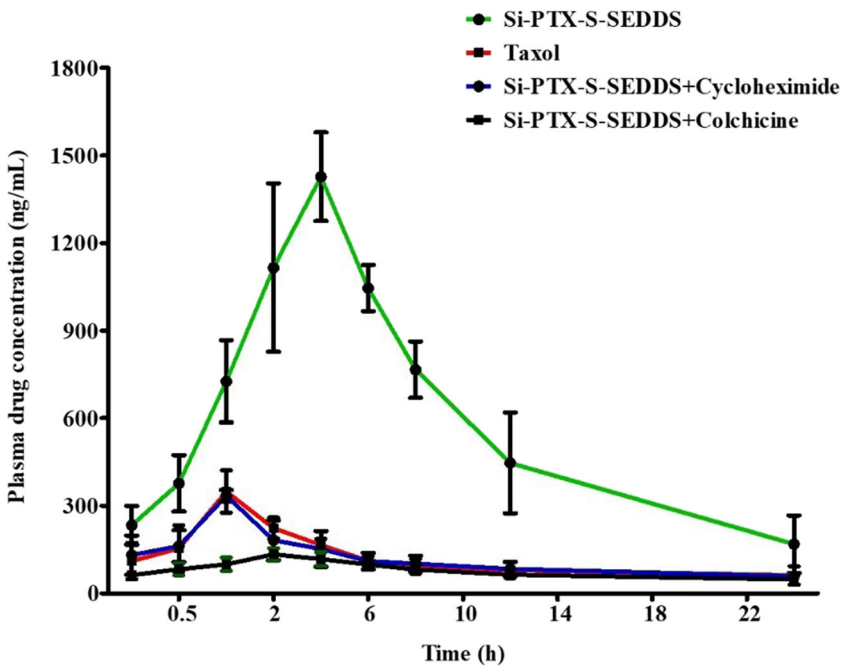

Fig. 6. Comparative plasma pharmacokinetic of PTX in Sprague Dawley rats after oral administration of Taxol and Si-PTX-S-SEDDS either alone or along with cycloheximide or colchicine

reduction in tumor burden in these two groups than control-treated animals where the weight was measured to be 13.29 ± 3.61 g. Tumor burden was also found to be significantly reduced in blank Si-S-SEDDS treatment group compared to control rats (p 0.05). Figure 7b exhibits the picture of excised tumor from all treatment groups.

Apoptosis in Tumor Tissues

TUNEL assay revealed that SEDDS formulation enhanced apoptotic activity of PTX compared to Taxol in the tumor tissues as shown in Fig. 7c. In the control-treated animals, tumor tissues showed intact cells with very low green fluorescence, whereas in the Taxol- and Si-PTX-S-SEDDS-treated rats, higher intensity of green fluorescence (TUNEL-positive) was seen. H&E stained tumor tissues on microscopic evaluation showed loosely arranged epithelial cells with very less number, necrotic areas and high stromal tissue in the Si-PTX-S-SEDDS treatment (Fig. 7d). Similar characteristics were seen in Taxol and in a lesser extent in the blank Si-S-SEDDS-treated animals. In these two groups, apoptotic cells were also visible and pyknotic hyperchromatic nuclei were seen indicating treatment-induced apoptosis. In contrast, the control-treated cells showed densely packed epithelial cells with very little connective tissues and mitotic marks along with high vasculature. All together these results corroborated the improved anticancer efficacy of PTX by the developed SEDDS formulation.

Lung Metastasis

Lung metastasis was studied by counting the metastatic count and also the histopathological changes (Fig. 7e and 7f). There was a significant (p 0.001) reduction in nodule count of animals treated with Si-PTX-S-SEDDS and Taxol compared to control group animals. Metastatic foci, neoplastic cells with higher mitotic activity, were seen in control-treated lung; however, in the Si-PTX-S-SEDDS- and Taxol-treated tissues, no such characteristics were observed.

DISCUSSION

Exploit of PTX for the pharmacotherapy of breast cancer is thwarted by profound drug delivery challenges,

Table V. Pharmacokinetic Parameters of Si-PTX-S-SEDDS After Oral Administration in Rats Alone and in Combination with Chylomicron Flow Inhibitors

PK parameters	Taxol (iv)	Si-PTX-S-SEDDS	Taxol (oral)	Si-PTX-S-SEDDS + Cycloheximide	Si-PTX-S-SEDDS + Colchicine
Dose (mg/kg)	10	20	20	20/3	20/5
T_{max} (h)	-	4.46 ± 0.59	1.14 ± 0.16[a]	1.60 ± 0.35[a]	1.67 ± 0.30[a]
C_{max} (ng/mL)	44,378.00 ± 8965.77	1627.00 ± 281.50	403.90 ± 78.02[a]	360.20 ± 37.08[a]	159.80 ± 37.50[a]
AUC (h.ng/mL)	31,460.00 ± 5887.34	16,071.00 ± 2580.00	2657.00 ± 208.80[a]	2572.00 ± 166.50[a]	1678.00 ± 145.40[a]
Bioavailability (%)	-	21.32 ± 1.86	4.28 ± 0.42[b]	4.39 ± 0.69[b]	3.54 ± 1.02[b]

PTX: PTX, [a] p 0.01, [b] p 0.001 (a, b; statistical significance difference is in comparison to Si-PTX-S-SEDDS) (mean ± SD; n = 3)

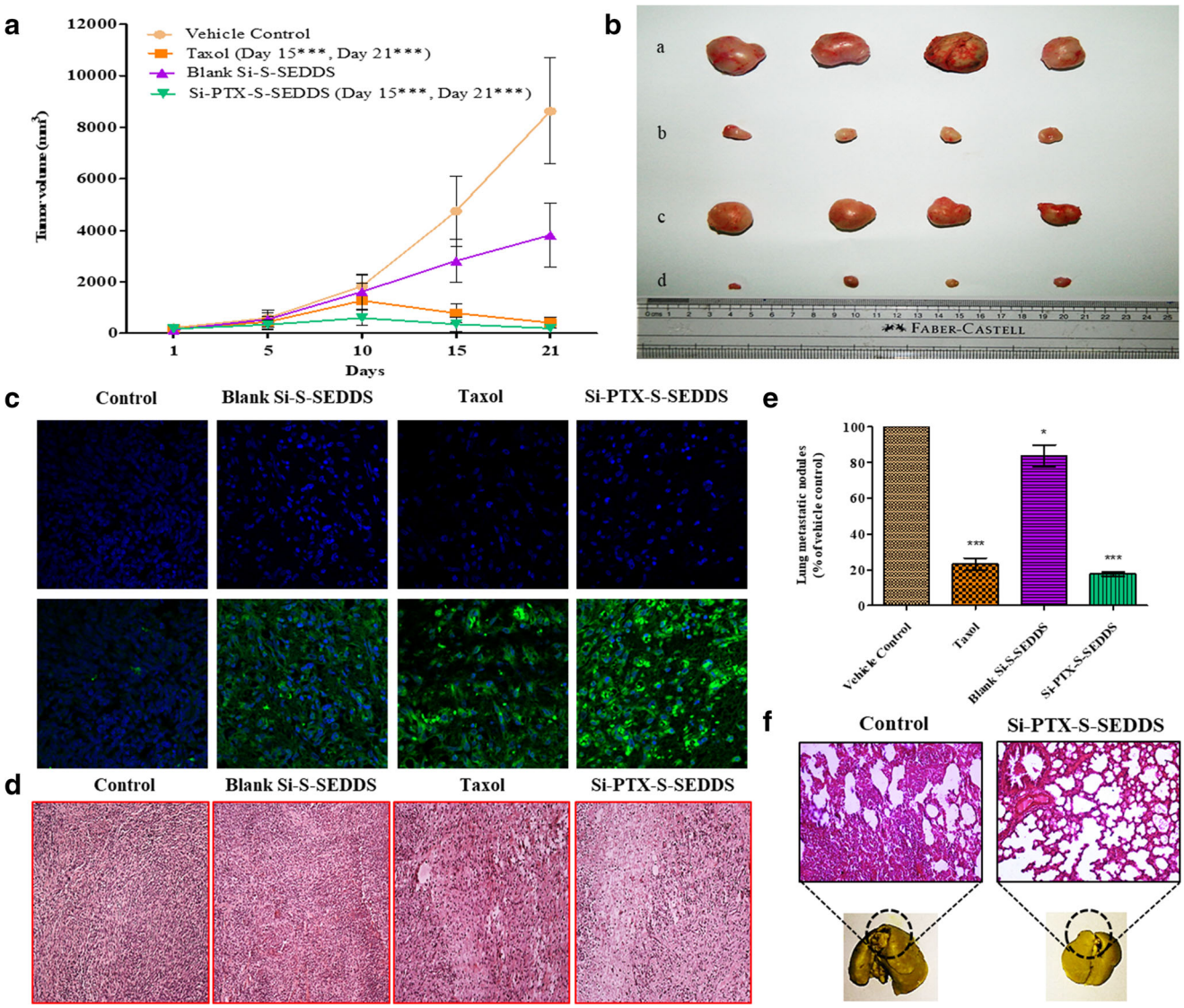

Fig. 7. *In vivo* anticancer activity against LA-7 syngeneic mammary tumor in SD rats. **a** Graph displaying change in tumor volume followed by various treatments over a period of 21 days. A significant reduction (***$p < 0.001$) in tumor volume was observed on 15th day of treatment and also seen on 21st day. **b** Representative photographs of excised tumors from (aa) control, (b) Taxol, (c) blank Si-S-SEDDS, and (d) Si-PTX-S-SEDDS treatment groups at the end of the study period. **c** TUNEL assay displaying apoptotic cells in tumor tissues detected as TUNEL-positive cells with high green fluorescence. **d** H&E staining showing alterations in the histopathological characteristics of tumor tissues after different treatments. **e** Lung metastasis study showing treatment-induced changes in the lung metastatic nodule count. There was a significant reduction (***$p < 0.001$) in metastatic nodule count in PTX-SEDDS-treated group than control and blank treatment. **f** Histopathological characteristics of lungs showing treatment-induced changes along with the lung images

owing to its extreme aversion to aqueous media. The marketed formulations further add to the affliction. Whether it is hypersensitivity, toxicity of the formulation's ingredients itself, patient incompliance, or even leaching from the PVC infusion bags, all these are serious concerns associated with the currently available PTX formulations and need some thoughtful attention (2). In all likelihood, oral delivery of PTX seems a plausible option in such situation but still this has been a farfetched dream for drug delivery scientists. There are many causatives responsible for such dire state, but the key one amongst them are poor aqueous solubility and p-gp efflux of PTX *via* the gut environment (8). In our present study, we have made an attempt to overcome these hurdles and deliver PTX *via* the oral route employing SEDDS formulations. SEDDS formulations have already proven their clinical efficacy and commercial significance as a pharmaceutical formulation for delivery of many drug molecules (Saquinavir, Tipranavir, and Cyclosporine) (20).

Being guided by the solubility studies for PTX as well as our prior understanding, we have selected a blend of vitamin E, TPGS, and Labrafac (3:1:1) as oil phase. Based on their contribution, the required HLB (rHLB) of the oil phase would be 6.44. To accommodate the oil phase in aqueous environment and to give rise to a stable emulsion system, Capryol® 90 and Gelucire® (4:1) were selected as a surfactant and co-surfactant system. Box-Behnken experimental design was employed to optimize the formulation. Feeding the experimental design, the range of dependent and

independent variables proposed a set of 17 runs with different combinations of the excipients. The formulations were developed and evaluated for droplet size and PDI. Experimental runs and the corresponding measured responses are shown in Table III. The mathematical relationship was derived between dependent and independent variables using a set of polynomial equations. The equation represents the interaction between independent variables (A: oil phase, B: Capryol®90, and C: Gelucire) and their quantitative effect on dependent variables (R_1: droplet size and R_2: PDI). The synergistic effect is represented by a positive sign and the antagonistic effect is indicated by a negative sign. The interaction between the independent and dependent variables was further illustrated by contour plots and 3D response surface plots (Fig. 1). When the concentration of surfactant was increased at a constant level of co-surfactants and low level of oil, the droplet size was significantly decreased. As we increased the amount of oil, similar trend was observed but droplet size was comparatively higher. In the case of the PDI, a similar trend was observed that at low concentration of oil, as we increased surfactant concentration at constant level of co-surfactants, the PDI decreased whereas at the high level of oil, PDI increased. The overall phenomenon might be due to the fact that only co-surfactant molecules surrounding the oil globules could reduce the interfacial tension to a certain extent that could not be sufficient to reduce the droplet size. However, as the surfactant concentrations increased progressively, a rigid interfacial surrounding layer could have been developed that was responsible for easy emulsification and reduction in droplet size of the oil droplets. The theoretical values of R_1 and R_2 were obtained by substituting the values of A, B, and C in polynomial equation given by the experimental design. The experimental design proposed a droplet size; 28.51, PDI; 0.124 at oil phase; 5.35, Capryol® 90; 11.94, and Gelucire; 3.00 with a desirability function of 1. The observed values were found to be in close agreement with the predicted (theoretical) values.

The conventional liquid SEDDS formulations are reported to have certain stability concerns and solid SEDDS have been found to be comparatively more stable and robust (21). In our study, we have developed fumed colloidal silica–based solid SEDDS (Si-PTX-S-SEDDS) by spray drying technique. The adopted method was simple and provides the privilege of scalability required for technology transfer to the industry. Furthermore, we have moved for pharmaceutical characterization of the developed solid SEDDS. DSC analysis revealed (Fig. 2a) conversion of the PTX from its native crystalline form to the amorphous form of PTX in the solid SEDDS, which was due to the encapsulation of the PTX into the core of oil-surfactant mixture. Conversion of PTX from crystalline form to amorphous form in delivery system was already anticipated from the previously reported studies (22). The emulsification time of the Si-PTX-S-SEDDS was found to be 1.5 ± 0.40 min and the ease in emulsification is attributed to the availability of optimum concentration of the surfactant and co-surfactant blend. Results derived from the laser diffraction study as well as from the topological/morphological analysis were in close agreement with each other and revealed round-shaped, uniformly dispersed particles of 2–3 μM size (Fig. 2). Upon reconstitution with aqueous media, the developed microparticles emulsified to fine globules in the range of 20–30 nm. Optimum concentration of the solid carrier as well as the optimized SEDDS formulation processed through a suitable formulation technique could result into the development of uniform microparticles. The smaller droplet size is also believed to cause in improved oral absorption and anticancer effect too. This particular topic is discussed in the subsequent section where the molecular insights have been discussed. Other pharmaceutical parameters like drug content, yield, and entrapment efficiency were in the acceptable range. *In vitro* drug release studies revealed diffusion type of controlled release of PTX from the nanoemulsion core (Fig. 2d). The release pattern of PTX from PTX-SEDDS was less than 50% after 48 h compared to Taxol with over 60% drug released from Taxol group in same period of time. The reason is that in Taxol the PTX is emulsified in ethanol and cremophor mixture and readily available for equilibrium with the release media, while the PTX in PTX-SEDDS formulation was intact inside the nanoemulsion core and not easily available for equilibrium with release media. This resulted in a sustained diffusion fashion due to the shielding effect of the amalgamated coat of oil and surfactant blend which make retarded release. This is further believed to be the reason for prolonged therapeutic benefit (23). Stability investigation revealed no significant alteration in the pharmaceutical parameters for a period of 6 months which is attributed to the simple formulation excipients admixture as well as solid state of the Si-PTX-SEDDS formulation (Table IV).

After studying pharmaceutical parameters, we have evaluated the solid SEDDS formulation for anticancer efficacy in cancer cell lines. Cytotoxicity assay of Si-PTX-S-SEDDS against MDA-MB-231 and MCF-7 exhibited higher toxicity than Taxol after 72 h of exposure (Fig. 3c). These findings were further substantiated by the results of cytomorphological investigations where both cellular and nuclear morphology exhibited higher cell death in the Si-PTX-S-SEDDS treatment than in Taxol treatment group (Fig. 3d and e). Cancer cells especially MDA-MB-231 are known to be an aggressive cell line that grows very fast. Wound healing assay revealed inhibition of cellular migration of MDA-MB-231cells upon treatment with the Si-PTX-S-SEDDS (Fig. 3f). All these are indicative of efficient cytotoxic potential of solid SEDDS formulation. Other more précised anticancer evaluation parameters investigated were cell cycle distribution, apoptosis, MMP, and ROS generation (Fig. 5). The cell cycle distribution study revealed G_2M phase arrest by the Si-PTX-S-SEDDS; however, the blank formulation showed G_0/G phase arrest (Fig. 5a). The increased MMP and higher ROS generation further potentiated the higher anticancer effect of Si-PTX-S-SEDDS (Fig. 5c and d), altogether leading to higher apoptotic population in Si-PTX-S-SEDDS treatment group compared to Taxol treatment group (Fig. 5b). The higher cytotoxic effect is due to the additive effect of functional excipients, *viz* vitamin E and TPGS, which are also reported to cause cytotoxicity in cancer cell line (8,24). Apart from this, nanoemulsion-assisted increase in cellular uptake of PTX is also responsible for the same. Cellular uptake of Si-PTX-S-SEDDS by MDA-MB-231 was found to be 45.83-fold higher than control cells that advocates the higher availability of drug at the cellular level for higher cytotoxicity (Fig. 4a and b). This enhanced cellular internalization of PTX by the

nanoemulsion can be explained by well-known phenomena associated with nano droplets like pinocytosis, caveolae, and dynamin-mediated cellular uptake, altogether leads to high payload delivery of PTX inside cancer cells and enhanced cytotoxicity.

As discussed in the "Results" section, there were significant alterations in the expression of various proteins after treatment of MDA-MB-231 cells with Si-PTX-S-SEDDS formulations. The pro-apoptotic protein Bax was increased significantly than the control treatment and at the same time the Bcl2, *i.e.*, anti-apoptotic protein, was seen to be decreased in a significant manner. So overall the Bax/Bcl2 ratio was observed to be in a decreasing trend. The Bax and Bcl2 proteins are from the Bcl2 family, where the Bax and Bak are known as the apoptosis activator proteins whereas the Bcl2 and Bcl-x_L are the apoptosis inhibitor proteins. The ratio of Bax/Bcl2 determines the fate of cells towards apoptosis. Furthermore, Bax is associated with the release of cytochrome c to the cytosol which binds to the activated caspase 9. Consequently, the association of Apaf causes formation of apoptosomes. Apoptosomes are the main machinery in activating the caspase 3 that ultimately leads to apoptosis (25). In our study, we could witness a significant upregulation of cleaved caspase 3 by the Si-PTX-S-SEDDS formulation, which is supposed to follow the abovementioned pathway in causing enhanced apoptosis in MDA-MB-231 cells. Both the PTX and TPGS are found responsible for such massive cytotoxicity leading to apoptosis that is in all cases higher than Taxol treatment (26).

In order to understand the upstream pathway responsible for treatment-induced apoptosis, we have investigated the Akt-mTOR pathway that is known to be activated by PTX (27). For the maintenance of cell growth and its progression either in terms of proliferation, growth, survival, or motility, the Akt-mTOR pathway plays a very crucial role and in many human cancers, it is known to be over activated. This might be the reason for uncontrolled proliferation and reduced apoptosis by the cancer cells (28). Akt is a serine/threonine protein kinase and it is known to be the down-stream effector of PI3K. In several human cancers, Akt is hyper activated owing to different factors like oncogenic factors, hormonal factors (androgen and estrogen), and angiogenic factors. Our present investigation showed both Akt and phosphorylated Akt were downregulated in the Si-PTX-S-SEDDS formulation–treated cells that caused enhanced apoptosis. P-Akt is well established to play a role in the regulation of key proteins in cancer, *viz* Bcl2, Bax, and caspase 9; those are associated with cell apoptosis and proliferation (29). Phosphorylation of pro-caspase 9 and additionally its inactivation is accomplished by Akt inside the cells. The phosphorylated form pro-caspase 9 occupies the binding sites on Apaf-1, inhibiting further autocatalytic self-activation and transactivation of inactive pro-caspase 9 in the apoptosome complex (30).

This usually leads to hindrances in caspase 3–mediated apoptosis in cancer cells; however, as evident from our results that show significant downregulation of both p-Akt and Akt, this mechanism is nullified. Apart from the action of PTX being the active pharmaceutical ingredient, TPGS and vitamin E are also observed to be contributory in such molecular phenomena (24). Significantly better performance of solid SEDDS formulations than Taxol is deemed to be because of such functional and active excipients. mTOR, a conserved serine/threonine protein kinase, plays a crucial role in cancer progression by acting on both up- and down-stream of Akt. The Si-PTX-S-SEDDS caused a significant downregulation of both mTOR and p-mTOR which is in coherence with the alteration in Akt. Both the PTX and TPGS are shown to alter mTOR as evident from the work reported by researchers (31). So based on all these alterations in proteins associated with cancer, it could be said that PTX in its solid SEDDS formulations performed better to improve anticancer action.

Interestingly, it could be observed that in the Taxol treatment group, there was a significant increase in survivin, which has also been reported by many research groups (32). Survivin is a well-established member of inhibitor of apoptosis (IAP) family and it is reported to be over expressed in many human tumor cells. Survivin inhibits apoptosis by interfering with the activity of caspases as well as Bax- and Fas-associated apoptosis in cancer cells (33). The upregulation of survivin is considered to be a negative aspect in killing cancer cells and this might be a reason for its resistance. However, in the Si-PTX-S-SEDDS-treated cells, survivin was found to be significantly downregulated. The effect of TPGS and vitamin E is supposed to be responsible for the same and hence, the employment of these functional excipients is found to be effective in bringing apoptosis (34). Additionally, we have investigated the effect of formulation on p-gp, as its role is crucial in availability of PTX at both the cancer cells as well as in the interstitial environment. P-gp is an ATPase from ABC transporters family that works *via* an energy-dependent transmembrane pump system to efflux xenobiotics to enter the cells. P-gp is abundantly available in many parts of the living system including the epithelial cells of GI tract and cancer cells (35). PTX is a substrate for p-gp and this has been a reason for its poor bioavailability *via* oral route and poor efficacy which may also lead to drug resistance (36). To combat this situation, we have employed TPGS and vitamin E as therapeutic armory to fight against p-gp and enhance bioavailability as well as efficacy of PTX. Western blots of p-gp reveal that in the Si-PTX-S-SEDDS treatment group, MDA-MB-231 cells exhibited downregulation of p-gp significantly than the control cells. This has been attributed to the overall effect of our optimized formulations against cancer cells.

To further confirm the p-gp inhibition potential of the solid SEDDS formulations, we have investigated the Rhodamine 123 accumulation assay in cancer cells (Fig. 4b). Rhodamine 123 is a fluorescent dye and a substrate of p-gp, so its permeation and accumulation in cells indicates the p-gp inhibition capacity of the compound/formulation under investigation (15). We could find that MDA-MB-231 cells could accumulate rhodamine 123 after being treated with Si-PTX-S-SEDDS as well as the blank Si-S-SEDDS formulations. As PTX is a substrate of p-gp, its availability inside cells is hindered, and at this juncture the ability of formulation to inhibit p-gp is a positive sign towards the performance of PTX *via* solid SEDDS delivery system. The presence of TPGS and vitamin E is responsible for this phenomena and the proposed mechanism is through ATPase inhibition (37). With all these obtained results, we could find that molecular mechanism in

enhanced effect of PTX in cancer cells is due to the upregulation of pro-apoptotic proteins as well as tumor suppressors and the downregulation of anti-apoptotic proteins. Further p-gp efflux by vitamin E and TPGS is another mechanistic feature responsible for enhanced performance of PTX *via* oral route of administration.

After being encouraged by the *in vitro* molecular mechanistic insight in PTX's therapeutic effect *via* the Si-PTX-S-SEDDS, the oral absorption enhancement was investigated and explored. The expected mechanism for oral absorption of hydrophobic moieties/drugs is *via* entrapment by the bile salts in the GIT and further absorption through the enterocytes. Another postulation is lymphatic uptake of the hydrophobic moieties/drugs that can enhance the oral bioavailability by bypassing the hepatic exposure (37). As the SEDDS formulation is being equipped with triglycerides, vitamin E, and TPGS, we predicted the oral absorption *via* lymphatic pathway. Chylomicron flow blocking experiment is a very important and effective tool in studying the lymphatic dependent uptake of orally administered moieties. Chylomicron is a lipoprotein found in the endoplasmic reticulum of the enterocytes and responsible for transporting the dietary lipids *via* lymphatic pathway. In our study, we have employed cycloheximide and colchicine as the chylomicron flow blockers in rats and investigated the oral bioavailability of the Si-PTX-S-SEDDS formulation (Fig. 6). We could find that there was a 4–6-fold decrease in oral bioavailability of the same formulation in both the inhibitors treated animals. This indicated a role of chylomicron in oral absorption of Si-PTX-S-SEDDS formulation in rats.

Oral bioavailability of PTX *via* Si-PTX-S-SEDDS was approximately 4 times higher than the Taxol treatment. The delivery system that ultimately gets converted into nanoemulsion could increase the total surface area in the GI tract and made PTX available in a very wide area. Apart from this, the emulsified droplets containing PTX were supposed to be participating in the indigenous mechanism of gastrointestinal system of making mixed micelles. This phenomenon augments their dissolution and subsequently monomolecular lipid dissociation from the mixed micelles caused in higher bioavailability of PTX from Si-PTX-S-SEDDS. As Taxol is composed of Cremophor EL which is not orally absorbed and might be a responsible for poor oral bioavailability of PTX from Taxol.

All these findings discussed so far helped us to move for pre-clinical anticancer studies in animal model. For the *in vivo* anticancer studies, we have chosen syngeneic mammary tumor model in Sprague Dawley rats. The proposed model has various advantages, *viz* (i) single-cell tumor initiation and multi-lineage differentiation potential, (ii) prompt proliferation and self-renewal characteristics, (iii) transplantation ability, (iv) simplicity of tumor induction, and (v) their similarity in hormone sensitivity and histology to human breast cancer (38). As described in the experimental part after the development of the tumor, animals were treated with various dosage regimens and anti-tumor efficacy was evaluated. A significant reduction in the tumor weight and volume in the Si-PTX-S-SEDDS-treated animals was observed (Fig. 7a and b), attributed to the improved bioavailability as well as additive effect of vitamin E and TPGS in the formulation. The developed blank delivery system also showed significant anticancer activity compared to vehicle control group owing to the use of TPGS as excipient which possess anticancer activity of its own (39). Apoptosis in tumor tissues was evident from the higher number of TUNEL-positive cells in the formulation treated tumor (Fig. 7c). These findings were further supported by the tumor histopathology results where the treated tissues exhibited necrotic areas, loosely arranged epithelial cells, large amount of stromal tissue, and pyknotic and hyperchromatic nuclei (Fig. 7d). Metastatic lung is frequently observed in breast cancer animal models and hence, this has been investigated. There was a marked reduction in metastatic nodule count in lungs of SD rats under treatment with Si-PTX-S-SEDDS (Fig. 7e). Histopathological evaluation of lung in tumor-bearing animals confirmed the above findings, where treated cells exhibited presence of less number of neoplastic cells in comparison to the control cells (Fig. 7f). All these effects are because of multiple factors such as availability of PTX in adequate concentration at the desired site, as well as additional effect of functional excipient that could potentiate the therapeutic efficacy of the PTX. So, the overall performance of Si-PTX-S-SEDDS was high and commendable in terms of safety and efficacy in breast cancer treatment.

CONCLUSION

Solid SEDDS of colloidal silica containing PTX and comprising vitamin E and TPGS as functional excipients was successfully formulated and optimized by employing experimental design. Enhanced cytotoxicity, apoptosis, mitochondrial membrane potential disruption, and ROS generation were achieved with the solid Si-PTX-S-SEDDS in comparison to Taxol. Upregulation of pro-apoptotic proteins and the downregulation of anti-apoptotic proteins in cancer cell lines were key points in molecular mechanistic studies that delineated mitochondria-mediated intrinsic pathway of apoptosis following Akt/mTOR pathway. Survivin downregulation by solid SEDDS was a significant achievement of the formulation as Taxol was observed to cause in upregulation of the same. Oral bioavailability of PTX from solid SEDDS in SD rats was approximately 4-fold higher than Taxol which was supported by lymphatic uptake of PTX. P-gp inhibition by the developed solid SEDDS formulation was further found to be an important cause in better efficacy. These were also reflected in *in vivo* anti-tumor studies where the solid SEDDS exhibited higher therapeutic efficacy in mammary tumor of SD rats. Overall, the solid SEDDS performed very effectively and safely in its aim towards treatment of breast cancer in animal model.

ACKNOWLEDGMENTS

All authors are thankful to Director CSIR-CDRI for providing all necessary infrastructure facility to conduct this research work. We are thankful to the staff of SAIF Division, CSIR-CDRI for their contributions in CLSM and FACS studies. This is CSIR-CDRI communication 10137.

FUNDING

This work was supported by funding from the Department of Biotechnology, Government of India [BT/PR14769/NNT/28/996/2015].

COMPLIANCE WITH ETHICAL STANDARDS

The pharmacokinetic studies of Si-PTX-S-SEDDS were carried out in Female Sprague Dawley rats (220–250 g) with prior approval from institutional animal ethics committee, CSIR-CDRI, Lucknow, India.

Conflict of Interest The authors declare that they have no conflict of interest.

REFERENCES

1. Price KS, Castells MC. Taxol reactions. Allergy Asthma Proc. 2002;23(3):205–8.
2. Kim SC, Yoon HJ, Lee JW, Yu J, Park ES, Chi SC. Investigation of the release behavior of DEHP from infusion sets by paclitaxel-loaded polymeric micelles. Int J Pharm. 2005;293(1–2).
3. Sun B, Pokhrel S, Dunphy DR, Zhang H, Ji Z, Wang X, *et al.* Reduction of acute inflammatory effects of fumed silica nanoparticles in the lung by adjusting silanol display through calcination and metal doping. ACS Nano. 2015;9(9).
4. Mennini N, Furlanetto S, Cirri M, Mura P. Quality by design approach for developing chitosan-Ca-alginate microspheres for colon delivery of celecoxib-hydroxypropyl-β-cyclodextrin-PVP complex. Eur J Pharm Biopharm. 2012;80(1).
5. Seo YG, Kim DH, Ramasamy T, Kim JH, Marasini N, Oh YK, *et al.* Development of docetaxel-loaded solid self-nanoemulsifying drug delivery system (SNEDDS) for enhanced chemotherapeutic effect. Int J Pharm. 2013;452(1–2).
6. Verma RK, Singh AK, Mohan M, Agrawal AK, Verma PRP, Gupta A, *et al.* Inhalable microparticles containing nitric oxide donors: saying NO to intracellular *Mycobacterium tuberculosis*. Mol Pharm. 2012;9(11).
7. Khan F, Islam MS, Roni MA, Jalil RU. Systematic development of self-emulsifying drug delivery systems of atorvastatin with improved bioavailability potential. Sci Pharm. 2012;80(4).
8. Pawar VK, Panchal SB, Singh Y, Meher JG, Sharma K, Singh P, *et al.* Immunotherapeutic vitamin e nanoemulsion synergies the antiproliferative activity of paclitaxel in breast cancer cells via modulating Th1 and Th2 immune response. J Control Release. 2014;196:295–306.
9. Ahmad N, Banala VT, Kushwaha P, Karvande A, Sharma S, Tripathi AK, *et al.* Quercetin-loaded solid lipid nanoparticles improve osteoprotective activity in an ovariectomized rat model: a preventive strategy for post-menopausal osteoporosis. RSC Adv. 2016;6(100).
10. Chavan RB, Modi SR, Bansal AK. Role of solid carriers in pharmaceutical performance of solid supersaturable SEDDS of celecoxib. Int J Pharm. 2015;495(1).
11. Kale AA, Patravale VB. Design and evaluation of self-emulsifying drug delivery systems (SEDDS) of nimodipine. AAPS PharmSciTech. 2008;9(1).
12. Gursoy N, Garrigue JS, Razafindratsita A, Lambert G, Benita S. Excipient effects on in vitro cytotoxicity of a novel paclitaxel self-emulsifying drug delivery system. J Pharm Sci. 2003;92(12).
13. Adams LS, Phung S, Yee N, Seeram NP, Li L, Chen S. Blueberry phytochemicals inhibit growth and metastatic potential of MDA-MB-231 breast cancer cells through modulation of the phosphatidylinositol 3-kinase pathway. Cancer Res. 2010;70(9).
14. Yang XH, Sladek TL, Liu X, Butler BR, Froelich CJ, Thor AD. Reconstitution of caspase 3 sensitizes MCF-7 breast cancer cells to doxorubicin- and etoposide-induced apoptosis. Cancer Res. 2001;61(1).
15. Jouan E, Le Vée M, Mayati A, Denizot C, Parmentier Y, Fardel O. Evaluation of P-glycoprotein inhibitory potential using a rhodamine 123 accumulation assay. Pharmaceutics. 2016;8(2).
16. Wang Z, Dong B, Feng Z, Yu S, Bao Y. A study on immunomodulatory mechanism of Polysaccharopeptide mediated by TLR4 signaling pathway. BMC Immunol. 2015;16(1).
17. Huang S, Shao K, Kuang Y, Liu Y, Li J, An S, *et al.* Tumor targeting and microenvironment-responsive nanoparticles for gene delivery. Biomaterials. 2013;34(21).
18. Wieder R. TUNEL assay as a measure of chemotherapy-induced apoptosis. Methods Mol Med. 2005;111.
19. Choi YJ, Nam SJ, Son MJ, Kim DK, Kim JH, Yang JH, *et al.* Erlotinib prevents pulmonary metastasis in curatively resected breast carcinoma using a mouse model. Oncol Rep. 2006;16(1).
20. Meher, J.G. *et al*. Self-emulsifying drug delivery systems: a novel drug delivery model. Oral modified release drug delivery systems. In: P. Khare, M. Chaurasia and SKP, editor. PharmaMed Press: a unit of BSP Books Pvt Ltd Hyderabad, India. Hyderabad: PharmaMed Press: A unit of BSP Books Pvt. Ltd.; 2018.
21. Kohli K, Chopra S, Dhar D, Arora S, Khar RK. Self-emulsifying drug delivery systems: an approach to enhance oral bioavailability. Vol. 15, Drug Discovery Today. 2010.
22. Mu L, Feng SS. A novel controlled release formulation for the anticancer drug paclitaxel (Taxol®): PLGA nanoparticles containing vitamin E TPGS. J Control Release. 2003;86(1).
23. Gupta R, Shea J, Scafe C, Shurlygina A, Rapoport N. Polymeric micelles and nanoemulsions as drug carriers: therapeutic efficacy, toxicity, and drug resistance. J Control Release. 2015;212:70–7.
24. Guo Y, Luo J, Tan S, Otieno BO, Zhang Z. The applications of vitamin e TPGS in drug delivery. European Journal of Pharmaceutical Sciences. 2013;49:175–86.
25. Riedl SJ, Salvesen GS. The apoptosome: signalling platform of cell death. Nature Reviews Molecular Cell Biology. 2007;8.
26. Varma MVS, Panchagnula R. Enhanced oral paclitaxel absorption with vitamin E-TPGS: effect on solubility and permeability in vitro, in situ and in vivo. Eur J Pharm Sci. 2005;25(4–5).
27. Blanco E, Sangai T, Wu S, Hsiao A, Ruiz-Esparza GU, Gonzalez-Delgado CA, *et al*. Colocalized delivery of rapamycin and paclitaxel to tumors enhances synergistic targeting of the PI3K/Akt/mTOR pathway. In: Molecular therapy. 2014
28. Vivanco I, Sawyers CL. The phosphatidylinositol 3-kinase-AKT pathway in humancancer. Nat Rev Cancer. 2002;2(7).
29. Xu N, Lao Y, Zhang Y, Gillespie DA. Akt: A double-edged sword in cell proliferation and genome stability. Journal of Oncology. 2012.
30. Cardone MH, Roy N, Stennicke HR, Salvesen GS, Franke TF, Stanbridge E, *et al.* Regulation of cell death protease caspase-9 by phosphorylation. Science (80-). 1998;282(5392).
31. Zou H, Li L, Carcedo IG, Xu ZP, Monteiro M, Gu W. Synergistic inhibition of colon cancer cell growth with nanoemulsion-loaded paclitaxel and PI3K/ mTOR dual inhibitor BEZ235 through apoptosis. Int J Nanomedicine. 2016;11.
32. Lu J, Tan M, Huang WC, Li P, Guo H, Tseng LM, *et al.* Mitotic deregulation by survivin in ErbB2-overexpressing breast cancer cells contributes to taxoI resistance. Clin Cancer Res. 2009;15(4).
33. Shin S, Sung BJ, Cho YS, Kim HJ, Ha NC, Hwang JI, *et al.* An anti-apoptotic protein human survivin is a direct inhibitor of caspase-3 and -7. Biochemistry. 2001;40(4).
34. Zhang Z, Feng SS. Nanoparticles of poly(lactide)/vitamin E TPGS copolymer for cancer chemotherapy: synthesis, formulation, characterization and in vitro drug release. Biomaterials. 2006;27(2).
35. Raghava KM, Lakshmi PK. Overview of P-glycoprotein inhibitors: a rational outlook. Vol. 48, Brazilian Journal of Pharmaceutical Sciences. 2012.
36. Jang SH, Guillaume Wientjes M, Au JLS. Kinetics of P-glycoprotein-mediated efflux of paclitaxel. J Pharmacol Exp Ther. 2001;298(3).
37. Collnot EM, Baldes C, Schaefer UF, Edgar KJ, Wempe MF, Lehr CM. Vitamin e TPGS P-glycoprotein inhibition mechanism: influence on conformational flexibility, intracellular ATP levels, and role of time and site of access. Mol Pharm. 2010;7(3).

38. Cocola C, Sanzone S, Astigiano S, Pelucchi P, Piscitelli E, Vilardo L, *et al*. A rat mammary gland cancer cell with stem cell properties of self-renewal and multi-lineage differentiation. In: Cytotechnology. 2008
39. Zhao L, Feng SS. Enhanced oral bioavailability of paclitaxel formulated in vitamin E-TPGS emulsified nanoparticles of biodegradable polymers: in vitro and in vivo studies. J Pharm Sci. 2010;99(8).